EM Scattering from Conducting Bodies using Non-Orthogonal Locally-One-Dimensional FDTD

Md. Masud Rana and M. A. Motin
Department of Electrical and Electronic Engineering
Rajshahi University of Engineering &Technology (RUET)
Rajshahi, Bangladesh,
Email: masud_01119e@yahoo.com, md.masud.rana.ruet@gmail.com

***Abstract*—In this paper, nonorthogonal locally one dimensional finite difference time domain (LOD-NFDTD) method based on curvilinear coordinate system is presented for analyzing electromagnetic scattering from curved conducting structures. A formulation of LOD-NFDTD method for two dimensional problems is provided. In our generalized approached, the non-orthogonal grid is used to model the computational domain which is bounded at the far end by a curvilinear convolutional perfectly matched layer (CPML) absorbing boundary condition. Numerical results are presented comparing with results available in the literature for TE_z scattering by conducting cylinders.**

Keywords—locally one dimensional (LOD); finite difference difference time domain (FDTD); non-orthogonal coordinates; CPML truncation; scattering.

I. Introduction

The finite-difference time-domain (FDTD) method is an explicit time domain technique which has been extensively applied for analysing many electromagnetic problems. The FDTD method is based on staggered central differencing in space and centred leapfrog integration in time (Yee scheme). For modelling objects with complicated geometries with the use of the Yee algorithm [1], a common approach is to employ staircasing to model the curved surfaces. However, when this procedure is used to analyse problems with complicated geometries, very fine grids are needed to obtain accurate results. Several techniques have been proposed to accurately model the complex structure with curved boundaries, including the conformal FDTD approach that uses conformal grids to model the boundary between two media. Alternate FDTD formulations that can accurately model the curved surfaces are also available [2]-[3]. The non-orthogonal FDTD (NFDTD) method is a standard generalized FDTD algorithm based on the non-orthogonal curvilinear coordinate system [4]-[7], as far as curved geometries are concerned, the NFDTD algorithm has demonstrated improved efficiency over conventional Yee's algorithm, due to the fact that considerably fewer cells are needed in the former by using conformal meshes instead of employing staircase approximation. However, these NFDTD schemes [4]-[7] are based on an explicit finite difference algorithm that needs to satisfy the Courant-Friedrich-Lewy (CFL) condition. As a result, a fine time step is required when fine grids are used, causing the computational time to increase dramatically. To overcome the CFL limitation, the unconditionally stable FDTD based on alternating direction implicit (ADI) has been developed [8]. However, the ADI-FDTD method still suffers for CFLN limitation and may not provide efficient performance for EM scattering problems. CFLN is defined by $\Delta t/\Delta t_{CFL}$ where Δt_{CFL} is determined from CFL condition. To avoid problem with CFLN, locally one dimensional FDTD was proposed [9]. The locally one dimensional finite-difference time-domain (LOD-FDTD) method is a new implicit FDTD scheme that can effectively solve problems related to electromagnetic scattering [10]-[13]. Unlike the standard FDTD method, LOD-FDTD method does not require satisfying the CFL stability constraint. Hence, in LOD-FDTD method, maximum time step size is not limited by the minimum cell size within the computational domain, which enables it to simulate the scattering problems with higher computational efficiency. Although curvilinear non-orthogonal grid methods were developed for standard FDTD and ADI-FDTD methods [13]-[14], thus far, only in [15], nonorthogonal grids were developed for LOD-FDTD method but most of cases orthogonal grids have been used for LOD-FDTD method. Hence, in this paper, we present generalized 2-D TE_z LOD-NFDTD in detail and also discuss the formulation of CPML absorbing boundary condition. Some representative numerical results are provided to validate the technique

II. Formulation of LOD-NFDTD

A. LOD-FDTD Method

For the wave propagation in an isotropic lossy medium, the Maxwell's equations can be written as:

$$\varepsilon \frac{\partial \vec{E}}{\partial t} + \sigma_e \vec{E} = \nabla \times \vec{H} \tag{1a}$$

$$-\mu \frac{\partial \vec{H}}{\partial t} - \sigma_m \vec{H} = \nabla \times \vec{E} \tag{1b}$$

where $(\vec{E}, \vec{H})$ are, respectively, the electric and magnetic field intensities and σ_e, σ_m are electric conductivity and equivalent magnetic loss, respectively. For the case of orthogonal locally one dimensional (LOD) FDTD method, each explicit time step must be changed to an implicit time step using two procedures. To get LOD-FDTD equations from

the above two equations, the field components will be moved forwarded each half time step only in the x, y and z direction. Now, we will cast the above equations in a generalized curvilinear co-ordinate (non-orthogonal) system.

B. LOD-NFDTD Formulation for 2-D TE_z Case

The non-orthogonal LOD FDTD algorithm is formulated using the covariant and contra-variant components of the electric and magnetic fields. More specifically, a system of general non-orthogonal curvilinear co-ordinates (u^1, u^2, u^3) in three dimensions can be characterized by a set of basis vectors $\mathbf{A}^i$ (i =1, 2, 3), where the differential of the position vector $\mathbf{r}$ is described as

$$d\mathbf{r} = \sum_{i=1}^{3} \frac{\partial \mathbf{r}}{\partial u^i} \partial u^i = \sum_{i=1}^{3} \mathbf{A}_i du^i == \sum_{i=1}^{3} \mathbf{A}^i du_i \tag{2}$$

These bases are defined such that $\mathbf{A}_i \cdot \mathbf{A}^j = \delta_{ij}$, and the metric coefficients, g_{ij} and g^{ij} are introduced through the relation $\mathbf{A}_i \cdot \mathbf{A}_j = g_{ij}$ $\mathbf{A}^i \cdot \mathbf{A}^j = g^{ij}$, $i, j = 1, 2, 3$. For a good discussion on non-orthogonal co-ordinates systems consult references [1]-[4]. To deal with the electric and magnetic field quantities on such grids, two different local co-ordinate systems are used. Equation (1) can be applied for non-orthogonal co-ordinates as shown in [4]. The electric and magnetic fields equations for the first procedure of the LOD-NFDTD method are given below:

Sub-step 1:

$$\begin{aligned} E^1|^{n+1/2}_{i+1/2,j} &= aE^1|^{n}_{i+1/2,j} \\ &+ \frac{b}{du^2}\times\left(H_3|^{n+1/2}_{i+1/2,j+1/2} - H_3|^{n+1/2}_{i+1/2,j-1/2}\right) \\ &+ \frac{b}{du^2}\times\left(H_3|^{n}_{i+1/2,j+1/2} - H_3|^{n}_{i+1/2,j-1/2}\right) \end{aligned} \tag{3a}$$

$$\begin{aligned} H^3|^{n+1/2}_{i+1/2,j+1/2} &= cH^3|^{n}_{i+1/2,j+1/2} \\ &+ \frac{d}{\Delta u^2}\times\left(E_1|^{n+1/2}_{i+1/2,j+1} - E_1|^{n+1/2}_{i+1/2,j}\right) \\ &+ \frac{d}{\Delta u^2}\times\left(E_1|^{n}_{i+1/2,j+1} - E_1|^{n}_{i+1/2,j}\right) \end{aligned} \tag{3b}$$

Sub-step 2:

$$\begin{aligned} E^2|^{n+1}_{i,j+1/2} &= aE^2|^{n+1/2}_{i,j+1/2} \\ &- \frac{b}{du^1}\times\left(H_3|^{n+1/2}_{i+1/2,j+1/2} - H_3|^{n+1/2}_{i-1/2,j+1/2}\right) \\ &- \frac{b}{du^1}\times\left(H_3|^{n+1}_{i+1/2,j+1/2} - H_3|^{n+1}_{i-1/2,j+1/2}\right) \end{aligned} \tag{4a}$$

$$\begin{aligned} H^3|^{n+1}_{i+1/2,j+1/2} &= cH^3|^{n+1/2}_{i+1/2,j+1/2} \\ &- \frac{d}{du^1}\times\left(E_2|^{n+1/2}_{i,j+1/2} - E_2|^{n+1/2}_{i+1,j+1/2}\right) \\ &- \frac{d}{du^1}\times\left(E_2|^{n+1}_{i,j+1/2} - E_2|^{n+1}_{i+1,j+1/2}\right) \end{aligned} \tag{4b}$$

where, $a = (4\varepsilon - \sigma_e\Delta t)/(4\varepsilon + \sigma_e\Delta t)$, $b = 2\Delta t/\sqrt{g}(4\varepsilon + \sigma_e\Delta t)$, $c = (4\mu - \sigma_m\Delta t)/(4\mu + \sigma_m\Delta t)$, $d = 2\Delta t/\sqrt{g}(4\mu + \sigma\Delta t)$.

The covariant E_m, H_m and contra-variant E^m, H^m (m = 1, 2, 3), together with g, are taken to be the same as that given in [4]. The relationship between covariant fields H_m, and contra-variant fields H^m (m = 1, 2, 3) is given by $H_m = g_{m1}H^1 + g_{m2}H^2 + g_{m3}H^3$, $H^m = g^{m1}H_1 + g^{m2}H_2 + g^{m3}H_3$, where g_{ml} and g^{ml} (m, l = 1, 2, 3) are tensors as defined in [4]. Similar relation holds for E_m, and E^m. Here H^m and E^m (m = 1, 2, 3) are true field components. For 2-D TE_z case, $H_3 = H^3$, the $E^1|^{n+1/2}$, $H_3|^{n+1/2}$ in (3a) and $H^3|^{n+1/2}$, $E_1|^{n+1/2}$ in (3b) are defined as synchronous variables. Since (3b) cannot be calculated directly, simultaneous linear equations have to be formed for (3a) and (3b) by eliminating the synchronous variables $H_3|^{n+1/2}_{i+1/2,j+1/2}$ and $H_3|^{n+1/2}_{i+1/2,j-1/2}$. So placing (3b) in (3a), then, according to [4], desired covariant field component are averaged by known contra-variant fields to give a second order accurate approximation, we have the following equation:

$$\begin{aligned} &-\alpha_{11}E^1|^{n+1/2}_{i+1/2,j-1} \\ &+ (1+2\alpha_{11})E^1|^{n+1/2}_{i+1/2,j} - \alpha_{11}E^1|^{n+1/2}_{i+1/2,j+1} \\ &= aE^1|^{n}_{i+1/2,j} \\ &+ \frac{bc}{\Delta u^2}\times\left(H^3|^{n}_{i+1/2,j+1/2} - H^3|^{n}_{i+1/2,j-1/2}\right) \\ &+ \alpha_{11}\times\left(E_1|^{n}_{i+1/2,j+1} - E_1|^{n}_{i+1/2,j}\right) \\ &- \alpha_{11}\times\left(E_1|^{n}_{i+1/2,j} - E_1|^{n}_{i+1/2,j-1}\right) \\ &+ \frac{b}{\Delta u^2}\times\left(H^3|^{n}_{i+1/2,j+1/2} - H^3|^{n}_{i+1/2,j-1/2}\right) \end{aligned} \tag{5}$$

where, $\alpha_{11} = g_{11}(bd/\Delta u^2\Delta u^2)$. Equation (3b) can be calculated directly. Similarly from (4a) and (4b), by eliminating the $H_3|^{n+1}_{i+1/2,j+1/2}$ then the higher order approximation is omitted, we have

$$\begin{aligned} &-\beta_{22}E^2|^{n+1}_{i-1,j+1/2} \\ &+ (1+2\beta_{22})E^2|^{n+1}_{i,j+1/2} - \beta_{22}E^2|^{n+1}_{i+1,j+1/2}) \\ &= aE^2|^{n+1/2}_{i,j+1/2} \\ &- \frac{bc}{\Delta u^1}\times\left(H^3|^{n+1/2}_{i-1/2,j+1/2} - H^3|^{n+1/2}_{i+1/2,j+1/2}\right) \\ &- \frac{b}{\Delta u^1}\times\left(H^3|^{n+1/2}_{i+1/2,j+1/2} - H^3|^{n+1/2}_{i-1/2,j+1/2}\right) + \beta_{22} \\ &\times\left(E^2|^{n+1/2}_{i-1,j+1/2} - E^2|^{n+1/2}_{i,j+1/2} - E^2|^{n+1/2}_{i,j+1/2} + E^2|^{n+1/2}_{i+1,j+1/2}\right) \end{aligned} \tag{6}$$

Since the simultaneous linear equation (5) and (6) can be written in tri-diagonal matrix form, they can be solved efficiently.

C. CPML ABC for LOD-NFDTD Method

Convolutional perfectly matched layer (CPML) is highly effective in absorbing evanescent waves and signals with long time signature. Using the CPML, the boundaries can be placed closer to the objects in the problem space so that time and memory saving can be achieved. The CPML method maps the Maxwell's equation into a complex stretched coordinate space by making use of the complex frequency shifted (CFS) tensor.

$$S_{ei} = \kappa_{ei} + \frac{\sigma_{pei}}{\alpha_{ei} + j\omega\varepsilon_0},\ S_{mi} = \kappa_{mi} + \frac{\sigma_{pmi}}{\alpha_{mi} + j\omega\varepsilon_0}\ i = x, y, z \qquad (7)$$

where, S_{ei}, S_{mi} are the stretched coordinate metrics, and σ_{pei} and σ_{pmi} are the electric and magnetic conductivities of the terminating media. For brevity, in this paper we provide only one step for the explanation of the method for LOD-NFDTD CPML:

Sub-step 1:

$$\begin{aligned} E^1|^{n+1/2}_{i+1/2,j} &= aE^1|^{n}_{i+1/2,j} \\ &+ \frac{b}{\Delta u^2}\times\left(H_3|^{n+1/2}_{i+1/2,j+1/2} - H_3|^{n+1/2}_{i+1/2,j-1/2}\right) \\ &+ \frac{b}{\Delta u^2}\times\left(H_3|^{n}_{i+1/2,j+1/2} - H_3|^{n}_{i+1/2,j-1/2}\right) \\ &+ C_{\psi e^1}(i+1/2,\ j)\times\psi^{n}_{e_{12}}|^{n}_{i+1/2,j} \end{aligned} \qquad (8a)$$

$$\begin{aligned} H^3|^{n+1/2}_{i+1/2,j+1/2} &= cH^3|^{n}_{i+1/2,j+1/2} \\ &+ \frac{d}{\Delta u^2}\times\left(E_1|^{n+1/2}_{i+1/2,j+1} - E_1|^{n+1/2}_{i+1/2,j}\right) \\ &+ \frac{d}{\Delta u^2}\times\left(E_1|^{n}_{i+1/2,j+1} - E_1|^{n}_{i+1/2,j}\right) \\ &+ C_{\psi h^3}(i+1/2,\ j+1/2)\times\psi^{n}_{h_{32}}|^{n}_{i+1/2,j+1/2} \end{aligned} \qquad (8b)$$

where, $b = 2\Delta t/k(j)\sqrt{g}(4\varepsilon+\sigma_e\Delta t)$, $C_{\psi_{e1}} = \Delta t/\sqrt{g}(4\varepsilon+\sigma_e\Delta t)k(j)\Delta u^2$ and $d = 2\Delta t/\sqrt{g}(4\mu+\sigma\Delta t)$, $C_{\psi_{h3}} = \Delta t/\sqrt{g}(4\mu+\sigma\Delta t)k(j)\Delta u^2$ and

$$\psi_{e_{12}}|^{n}_{i+1/2,j} = b_r\psi_{e_{12}}|^{n-1/2}_{i+1/2,j} + a_r(H_3|^{n}_{i+1/2,j+1/2} - H_3|^{n}_{i+1/2,j-1/2}) \qquad (9)$$

$$\psi_{h_{32}}|^{n}_{i+1/2,j+1/2} = b_r\psi_{h_{32}}|^{n-1/2}_{i+1/2,j+1/2} + a_r(E_1|^{n}_{i+1/2,j+1} - E_1|^{n}_{i+1/2,j}) \qquad (10)$$

where, $a_r = \frac{\sigma_r}{(\sigma_r\kappa_r + \alpha_r\kappa_r^2)}[b_r - 1]$ and $b_{my} = e^{-(\frac{\sigma_{pmy}}{\kappa_{my}} + \alpha_{pmy})\Delta t/\varepsilon_0}$

In order to avoid reflections between the computational domain and the CPML boundary due to the discontinuity of s_{ei} and s_{mi}, the losses due to the CPML must be zero at the computational domain interface. Since (8a) and (8b), each contain one auxiliary ψ term, there are two ψ terms in step 1 and similarly two in step 2, whereas non-orthogonal ADI-CPML method requires four auxiliary terms in the first step and four in second. The lower number of auxiliary equations results in a higher computational efficiency of the non-orthogonal LOD-CPML. While the non-orthogonal FDTD-CPML also requires four auxiliary equations, it is more efficient than non-orthogonal LOD-CPML for the same CFLN, since only one simulation step is required for the temporal update of the fields.

III. Numerical Results

We shall now compare our numerical results for a circular cylinder. For conducting cylinder, we generate the curvilinear meshes as shown in Fig. 1. We assumed that a harmonic wave strikes the cylinder at time $\tau = 0$. For this geometry, steady state occurred in less than the total time required for the wave to traverse twice the maximum computational domain length. We present comparison of results at an average resolution of 15 points/wavelength away from the cylinder and 15 points/wavelength on the surface of the cylinder.

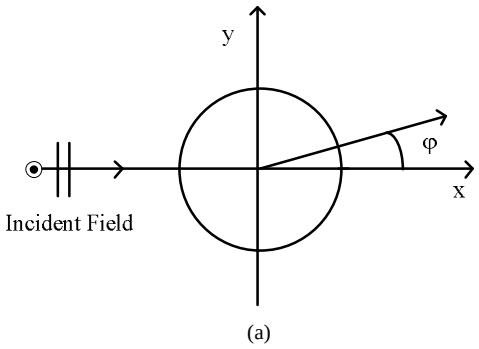

(a)

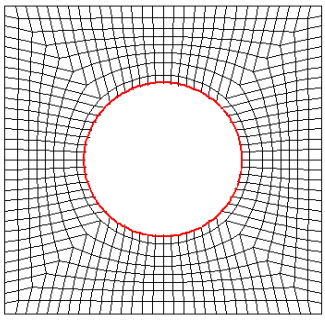

(b)

Fig. 1 (a) Plane wave incidence on conducting cylinder, (b) Nonorthogonal meshes of conducting cylinder.

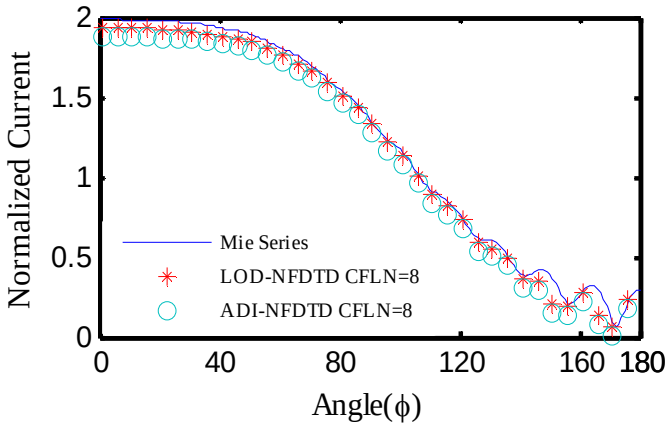

Fig.2 Bistatic scattering on the conducting circular cylinder (radius 1.6λ) for TE_z wave

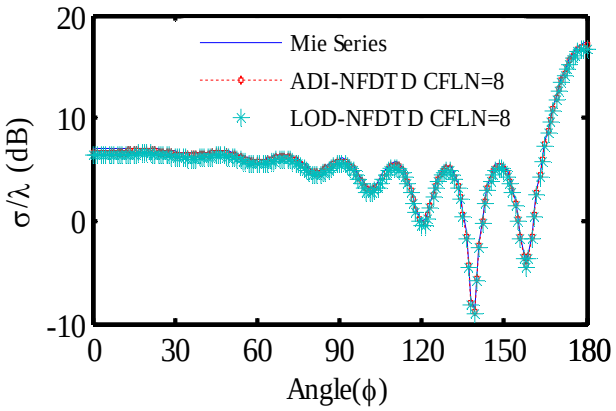

Fig.3. Bistatic scattering on the conducting circular cylinder (radius 1.6λ) for TE_z wave

In the ξ direction, our mesh is compressed near the surface of the cylinder and gradually becomes coarser. The ratio of the average to minimum cell length was equal to two. Within the CPML region, we have explored using various possibilities for the conductivity profiles. These included constant as well as tapered profiles such as linear, quadratic, and exponential. These profiles were modeled as

$$\sigma = \sigma_0 \varsigma^n \tag{11}$$

$(n = 0,\ 1,\ 2)$ respectively, in the case of the first three and as

$$\sigma = \sigma_0 \left(1 - \varsigma^n\right) \tag{12}$$

in the case of the exponential where the CPML region exists between $L \le \xi \le N_\xi$ and $\varsigma = (\xi - L)/(N_\xi - L)$. The constant σ_0 can be chosen to provide a preset attenuation $A(>1)$ dB in the CPML region

$$\int_{\text{PML region}} \sigma(\xi) d\ell_1 = \int_{\xi=L}^{N_\xi} \sigma(\xi) \sqrt{g_{11}}\, d\xi = A/8.686 \tag{13}$$

We have chosen a typical value of 30 dB for the attenuation A. We found that constant conductivity profile produced poorer results compared to the tapered profiles. There was some improvement in the solution in going from linear to quadratic. The exponential taper $n \ge 1$ provides a very smooth transition from a low σ to a high σ. However, the results did not differ much from the quadratic profile. In the subsequent results, our PML region extends over half a wavelength and we chose a quadratic conductivity profile with $\sigma_0 = 5$. Fig. 2 shows the magnitude of the normalized current for a circular cylinder of radius $a = 1.6\lambda$ $(ka = 10)$. The incident wave is assumed to propagate along the negative x axis. The PML region extended between $a + 2\lambda$ and $a + 2.5\lambda$. For the chosen resolution, we get a total of 150 points on the cylinder and 31 points along a ray. The PML region had seven layers. Time increment $\delta\tau$ was chosen to be 0.03 and the fields were marched over a length of time equal to one round trip travel over the computational domain. Fig. 3 shows results on the bistatic scattering width. It is seen that the agreement with the exact solution is quite good in both cases.

IV. Conclusion

In this paper, the LOD-NFDTD scheme is presented based on non-orthogonal coordinate system for analysing EM scattering from conducting bodies. Like ADI-FDTD and LOD-FDTD methods, the proposed scheme is free from the constraint of the CFL condition. Since the non-orthogonal gridding is useful for modelling the curved surfaces accurately, the proposed scheme can be gainfully employed for efficient computations of electromagnetic devices with complex geometries. Numerical results show that the new scheme is stable and can provide accurate results compared with the results in the literature.

References

[1] K. S. Yee, "Numerical solution of initial boundary value problems involving Maxwell's equation in isotropic media," *IEEE Trans. Antennas Propagat.*, vol. 14, pp.302-307, May 1966.

[2] W. Yu and R. Mittra, "A conformal finite difference time domain technique for modeling curved dielectric surfaces," *IEEE Microw. Wireless Compon. Lett.*, vol. 11, pp. 25-27, Jan 2001.

[3] A. Taflove and S. C. Hagness, *Computational electrodynamics- the finite-difference time-domain method*, Norwood, MA: Artech House, 2000.

[4] R. Holland, "Finite difference solution of Maxwell's equations in generalized nonorthogonal coordinates," *IEEE Trans. Nucl. Sci.*, vol. 30, no. 12, pp.4589-4591, Dec 1983.

[5] M. Fusco, "FDTD algorithm in curvilinear co-ordinates," *IEEE Trans. Antenna Propag.*, vol. 38, no. 1, pp. 76-89, Jan 1990.

[6] J. F. Lee, R. Palandech, and R. Mittra,"Modeling three dimensional waveguide discontinuties using FDTD algorithm in curvilinear coordinate system" *IEEE Trans. Microw. Theory Tech.*, vol. 40, no. 2, pp. 346-352, Feb 1992.

[7] P. H. Harms, J. F. Lee, and R. Mittra, "A study of the nonorthogonal FDTD method versus the conventional FDTD technique for computing resonant frequencies of cylindrical cavities," *IEEE Trans. Microw. Theory Tech.*, vol. 40, no. 4, pp. 741-746, April 1992

[8] T. Namiki, "A new FDTD algorithm based on alternating-direction implicit method," *IEEE Trans. Microw. Theory Tech..*, vol. 47, no. 10, pp. 2003-2007, Oct 1999.

[9] J. Shibayama, M. Muraki, J. Yamauchi, and H. Nakano, "Efficient implicit FDTD algorithm based on locally one dimensional scheme," *Electron. Lett.*, vol. 41, no. 19, pp. 1046-1047, Sep 2005.

[10] E. L. Tan, "Unconditionally stable LOD-FDTD method for 3-D Maxwell's equations," *IEEE Microw. Wireless Compon. Lett.*, vol. 17, no. 2, pp. 85-87, Feb 2007.

[11] M. M. Rana, and A. S. Mohan, "Convolutional perfectly matched layer ABC for 3-D LOD-FDTD using fundamental scheme," *IEEE Microw. Wireless Compon. Lett.*, vol. 23, no. 8, pp. 388–390, Aug. 2013.

[12] I. Ahmed, E. H. Khoo, and E. P. Li, "Development of the CPML for three-dimensional unconditionally stable LOD-FDTD method," *IEEE Trans. Antenna Propag.*, vol. 58, no.3, pp. 832-837, March 2010.

[13] H.-X. Zheng and K. W. Leung, "A nonorthogonal ADI FDTD algorithm for solving two dimensional scattering problems," *IEEE Trans. Antennas Propagat.*, vol. 57, no. 12, pp.3891-3902, Dec. 2009.

[14] H.-X. Zheng and K. W. Leung, "Three-dimensionally nonorthogonal alternating direction implicit finite-difference time-domain algorithm for full-wave analysis of microwave monolithic circuit devices," *IEEE Trans. Microw. Theory Tech.*, vol. 58, no. 1, pp.128-135, Jan. 2010.

[15] M. Rana, and A. S. Mohan, "Nonorthogonal LOD-FDTD method for EM scattering from two-dimensional structures," *IEEE Trans. Electromag. Compat*, vol. 55, no. 4, pp. 764–772, Aug., 2013.